Article

Cell

Vaginal Exposure to Zika Virus during Pregnancy Leads to Fetal Brain Infection

Graphical Abstract

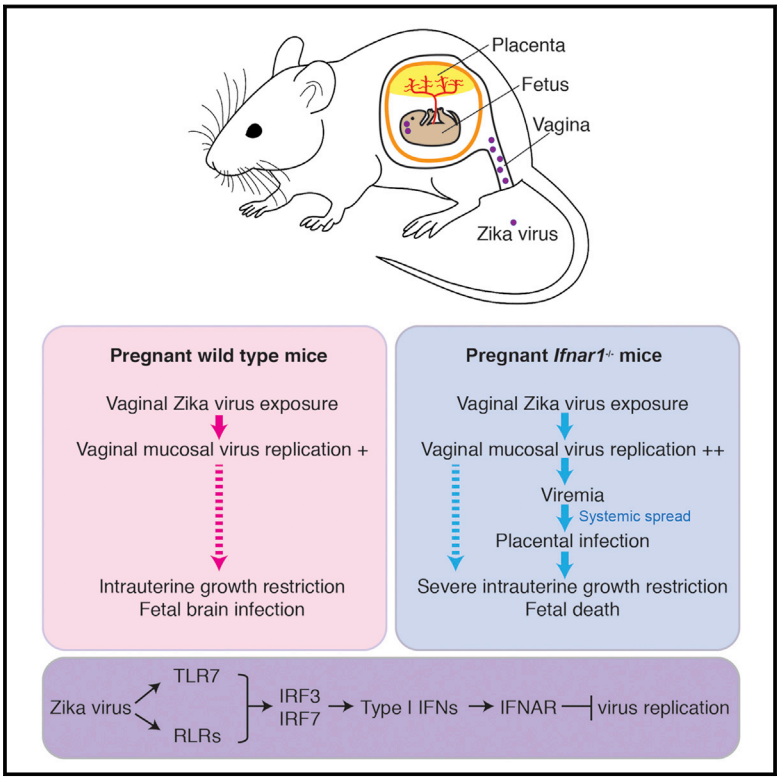

Highlights

- Zika virus replicates in the vaginal tract of wild-type virgin and pregnant mice
- Innate RNA sensors and type I interferons control vaginal Zika virus replication
- Vaginal Zika virus infection in early pregnancy leads to fetal growth restriction
- Vaginal Zika virus infection of pregnant dams leads to fetal brain infection

Authors

Laura J. Yockey, Luis Varela, Tasfia Rakib, ..., Brett D. Lindenbach, Tamas L. Horvath, Akiko Iwasaki

Correspondence

akiko.iwasaki@yale.edu

In Brief

Vaginal mucosa is permissive to the replication of Zika virus, and infection through this route can lead to fetal brain infection even in mice with an intact immune system.

Yockey et al., 2016, Cell *166*, 1247–1256
August 25, 2016 © 2016 Elsevier Inc.
http://dx.doi.org/10.1016/j.cell.2016.08.004

CellPress

Article

Cell

Vaginal Exposure to Zika Virus during Pregnancy Leads to Fetal Brain Infection

Laura J. Yockey,[1] Luis Varela,[2] Tasfia Rakib,[1] William Khoury-Hanold,[1] Susan L. Fink,[1,3] Bernardo Stutz,[2] Klara Szigeti-Buck,[2] Anthony Van den Pol,[4] Brett D. Lindenbach,[5] Tamas L. Horvath,[2] and Akiko Iwasaki[1,6,7,*]

[1]Department of Immunobiology
[2]Program in Integrative Cell Signaling and Neurobiology of Metabolism, Section of Comparative Medicine
[3]Department of Laboratory Medicine
[4]Department of Neurosurgery
[5]Department of Microbial Pathogenesis
[6]Howard Hughes Medical Institute
Yale University School of Medicine, New Haven, CT, 06520 USA
[7]Lead Contact
*Correspondence: akiko.iwasaki@yale.edu
http://dx.doi.org/10.1016/j.cell.2016.08.004

SUMMARY

Zika virus (ZIKV) can be transmitted sexually between humans. However, it is unknown whether ZIKV replicates in the vagina and impacts the unborn fetus. Here, we establish a mouse model of vaginal ZIKV infection and demonstrate that, unlike other routes, ZIKV replicates within the genital mucosa even in wild-type (WT) mice. Mice lacking RNA sensors or transcription factors IRF3 and IRF7 resulted in higher levels of local viral replication. Furthermore, mice lacking the type I interferon (IFN) receptor (IFNAR) became viremic and died of infection after a high-dose vaginal ZIKV challenge. Notably, vaginal infection of pregnant dams during early pregnancy led to fetal growth restriction and infection of the fetal brain in WT mice. This was exacerbated in mice deficient in IFN pathways, leading to abortion. Our study highlights the vaginal tract as a highly susceptible site of ZIKV replication and illustrates the dire disease consequences during pregnancy.

INTRODUCTION

While Zika virus (ZIKV) is well known for its transmission through the *Aedes* mosquitoes, recent evidence highlights another important route of transmission: through sexual contact with an infected partner. There have been multiple confirmed and suspected cases of sexual transmission in humans. Most of these reports involve transmission from infected men to their female partners (Foy et al., 2011; Hills et al., 2016; Lazear and Diamond, 2016; Mansuy et al., 2016; Petersen et al., 2016; Rowland et al., 2016; Venturi et al., 2016), but sexual transmission has also been reported from an infected man to a male partner (Deckard et al., 2016), and most recently from an infected woman to a male partner (Davidson et al., 2016). In addition, ZIKV has been detected in semen of infected men for as long as 62 days after initial symptoms (Mansuy et al., 2016; Musso et al., 2015; Rowland et al., 2016). ZIKV has also been detected in the cervical mucus and genital swab of a woman (Prisant et al., 2016), supporting the possibility of female to male sexual transmission. Collectively, these studies indicate that in humans, sexual transmission of ZIKV is possible from male to female, male to male, and female to male.

Pregnant women are at a higher risk for more severe complications following a wide range of viral infections. These viruses include influenza virus, hepatitis viruses, herpes viruses, rubella virus, human immunodeficiency virus-1 (HIV-1), Ebola virus and Lassa fever virus (Silasi et al., 2015). In addition, infants born to mothers infected with HIV-1, herpes simplex virus type 2, influenza virus, and human cytomegalovirus (CMV) during pregnancy have an increased risk for adverse outcomes. Infections of pregnant mothers with viruses such as rubella, CMV, and others have been shown to result in microcephaly of the fetus/infant. Multiple cases of babies born with microcephaly to ZIKV-infected mothers have reported the presence of ZIKV in the fetal brains (Driggers et al., 2016; Martines et al., 2016; Mlakar et al., 2016). However, the disease consequences on the fetus after sexual exposure of pregnant mothers to ZIKV are unknown.

The innate immune system detects viral infections through the recognition of molecular patterns that are specifically present or generated during infection. The best-characterized viral sensors are the pattern recognition receptors (PRRs), which detect invariant molecular patterns found in most microorganisms of a given class, known as pathogen-associated molecular patterns (PAMPs) (Janeway, 1989; Medzhitov, 2001). Distinct classes of viruses are recognized by distinct sets of PRRs (Takeuchi and Akira, 2007). Engagement of PRRs by viral PAMPs result in the transcriptional activation of cytokines downstream of the transcription factor NF-kB, and the type I interferon (IFN) genes downstream of IRF3 and IRF7 (Honda et al., 2006). Type I IFNs bind to their receptor IFNAR and induce hundreds of IFN-stimulated genes (ISGs) that work in combination to block viral replication and induce adaptive immune responses to the virus (Schoggins and Rice, 2011). In addition, many ISGs can be induced by signaling

downstream of PRRs through IRF3 and IRF7 (Honda and Taniguchi, 2006; Honda et al., 2005), independently of IFNAR signaling. The genome of flaviviruses (of which ZIKV is a member) is composed of positive-sense RNA. In plasmacytoid dendritic cells (pDCs), a specialized sensor of viruses that secrete large amounts of type I IFNs, Toll-like receptor 7 (TLR7) in the endosome recognizes the genomic RNA of the incoming virions and mounts antiviral responses to flaviviruses (Bruni et al., 2015; Décembre et al., 2014; Nazmi et al., 2014; Town et al., 2009; Wang et al., 2006; Welte et al., 2009). In contrast, the infected cells sense RNA virus infections by RIG-I (which recognizes 5′triphosphorylated dsRNA) and/or MDA5 (which recognizes long dsRNA), which are collectively known as the RIG-I-like receptors (RLRs). A subset of flaviviruses is recognized by both RIG-I and MDA5 (dengue, West Nile virus), while others are preferentially recognized by RIG-I (Japanese encephalitis virus, hepatitis C virus) (Foy et al., 2005; Loo et al., 2008; Saito et al., 2008). Of note, in mice deficient in mitochondrial antiviral-signaling proteins (MAVS), the signaling adaptor of RLRs, subcutaneous infection with ZIKV is well tolerated (Lazear et al., 2016), suggesting the presence of redundant sensors that trigger protective innate immune responses in mice. In addition, while cGAS is a cytosolic DNA sensor, it is required for innate defense against West Nile virus (Schoggins et al., 2014). However, which innate immune pathways are required to control vaginal transmission of ZIKV within the female host or within the fetus is unknown.

Recent studies using the mouse model of ZIKV have revealed that type I interferon (IFN) receptor (IFNAR) is critical in host resistance against ZIKV (Dowall et al., 2016; Lazear et al., 2016; Rossi et al., 2016) and that there is a persistent replication of the virus within the testes of IFNAR-deficient (*Ifnar1*$^{-/-}$) male mice (Lazear et al., 2016). Subcutaneous ZIKV infection of *Ifnar1*$^{-/-}$ dams mated with WT sires resulted in intrauterine growth restriction (IUGR) (Miner et al., 2016). While some have reported changes in fetal brain development after intraperitoneal infection of pregnant C57BL/6 mice (Wu et al., 2016), others found no apparent impact on either fetal brain size or fetal weight in this strain of mice injected intravenously (Cugola et al., 2016). One of the reasons why wild-type mice are resistant to ZIKV infection may be explained by the fact that ZIKV evolved to target human, but not mouse, STAT2 for degradation (Grant et al., 2016). Therefore, previous reports have used *Ifnar1*$^{-/-}$ mice or antibody treatment to block IFNAR to study ZIKV infection in mice (Dowall et al., 2016; Lazear et al., 2016; Rossi et al., 2016). However, virtually nothing is known about the pathogenesis of sexual ZIKV transmission and the defense mechanisms that prevent sexual transmission of ZIKV in women.

To this end, we developed a vaginal ZIKV transmission model in mice. We investigate viral replication in female mice that have genetic deletions in various innate sensors, adaptors, transcription factors, and the type I interferon receptor. Further, we examine the viral replication and disease consequences following vaginal infection of pregnant mice with ZIKV and examine viral transmission from infected dams to fetuses and its impact on fetal development.

RESULTS

ZIKV Replicates in the Vaginal Tract of Wild-Type Mice

It is unknown whether mice are susceptible to sexual transmission of ZIKV and, if so, what mechanisms are required to protect the host. To address this issue we established a mouse model of vaginal ZIKV infection. In other vaginal viral infection models, the diestrus phase of the estrus cycle renders the host susceptible to infection (Parr et al., 1994). To synchronize the estrus cycle of the female mice to the diestrus phase, mice were first injected with medroxyprogesterone acetate (Depo-Provera) 5 days prior to ZIKV vaginal challenge. Wild-type (WT) C57BL/6 virgin female mice were inoculated intravaginally (ivag) with 2.5×10^4 PFU of Cambodian ZIKV strain FSS13025. This strain is an Asian lineage of ZIKV isolated in 2010 from a pediatric case and is phylogenetically closely related to the ZIKV strains involved in the ongoing epidemic in the Americas (Grant et al., 2016; Haddow et al., 2012; Wang et al., 2016). Viral load in the vaginal wash was measured daily. Remarkably, viral RNA persisted in the majority of mice from days 1–4 post-infection and declined to undetectable levels in most mice by 7 days post-infection (dpi; Figure 1A). All of the ZIKV-infected C57BL/6 mice survived and showed no signs of weight loss (Figure 1B). To ensure that the viral RNA reflected infectious virus, we conducted viral plaque assays of the vaginal washes. Infectious viral particles were detected in the vaginal wash (Figure S1A) and correlated well (Spearman correlation of 0.85, $p < 0.0001$) with the viral RNA measured by RT-qPCR (Figure S1B). Based on the strong correlation between the viral RNA levels and the plaque forming units (Figure S1B), we decided to use viral RNA as a proxy for infectious virus throughout this study.

Our results indicated prolonged presence of ZIKV RNA (Figures 1A, S1C) and infectious virus (Figure S1A) in the vaginal mucosa following genital infection with ZIKV. To ensure that the persistent viral RNA and infectious particles did not reflect residual input virus, we examined an earlier time point of infection. We detected ZIKV RNA as early as 6 hr post-infection (Figure 1C). Importantly, the titers of ZIKV RNA were significantly elevated by 24 hr post-infection (Figure 1C). These results suggest that while only a small fraction of the input ZIKV successfully entered the host cells (6 hr), the virus has replicated in the subsequent 18 hr in the vaginal tissue.

Thus far, studies of ZIKV infection in adult WT mice have reported only low and transient viral RNA presence but no infectious virus following subcutaneous injections in vivo (Dowall et al., 2016; Lazear et al., 2016). However, the vaginal route of ZIKV infection supports productive replication in WT mice. To directly compare the levels of viral replication after vaginal versus systemic infection, we infected Depo-Provera-treated virgin WT mice either intravaginally (by using a pipette) or intraperitoneally (by using a needle). On 1 and 3 dpi, we collected spleens and vaginas to measure ZIKV RNA. These results indicated that intraperitoneal injection of ZIKV into WT mice resulted in extremely low levels of viral RNA found in the spleen 1 dpi and undetectable levels by 3 dpi (Figure 1D), consistent with previous studies (Dowall et al., 2016; Lazear et al., 2016). In contrast, ivag inoculation of ZIKV resulted in much higher levels of viral RNA detected in the vaginal mucosa on 1 and 3 dpi (Figure 1E).

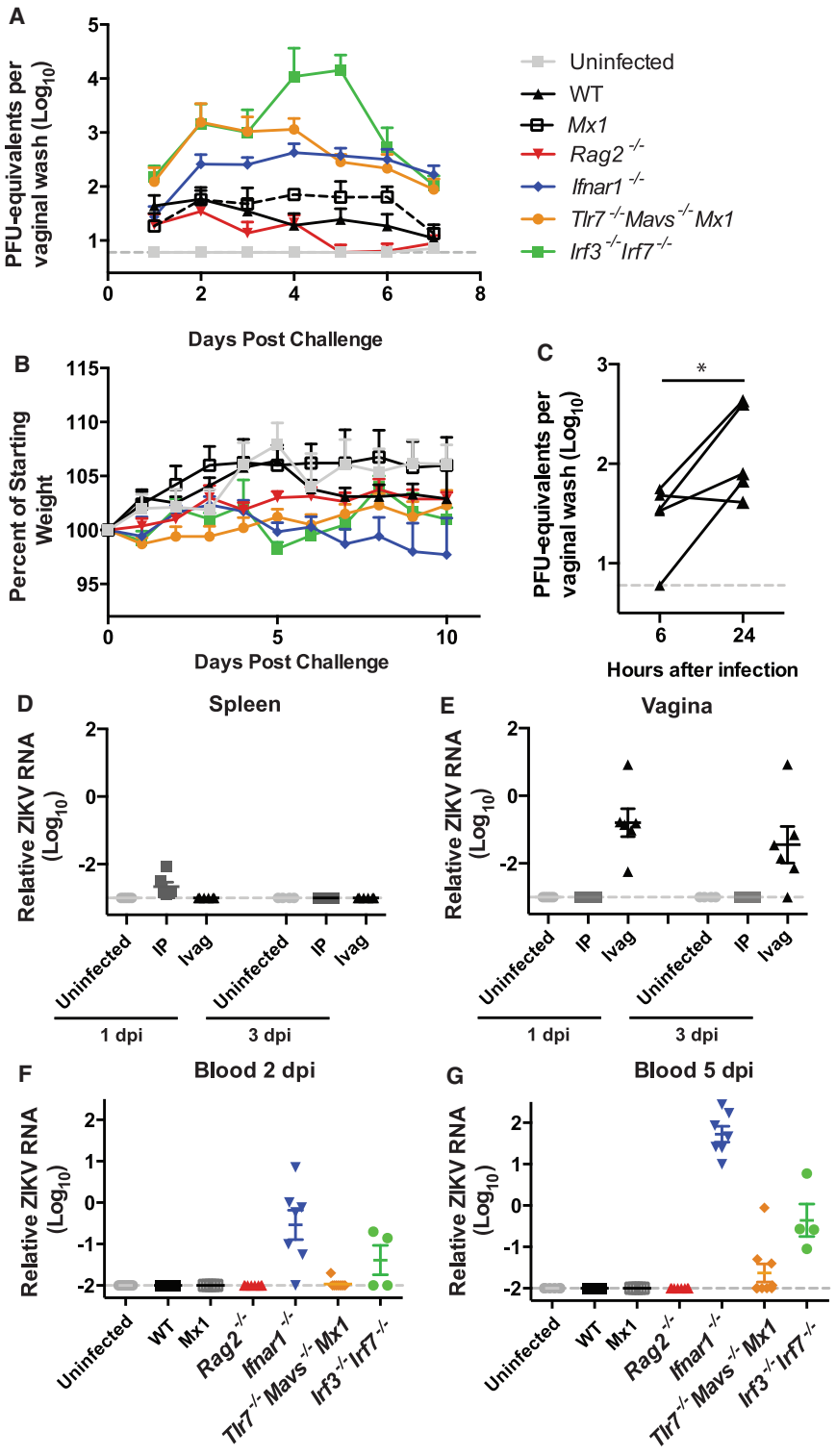

Figure 1. Vaginal Infection of Virgin Female Wild-Type Mice Leads to Viral Replication in the Vaginal Mucosa

(A and B) Seven- to 22-week-old Depo-Provera-treated virgin female mice of the indicated genotypes were infected intravaginally with 2.5×10^4 PFU of Cambodian ZIKV. (A) On the indicated days post-infection, vaginal washes were collected and viral load was analyzed by RT-qPCR. (B) Mice were weighed daily and represented as a percentage of starting weight.

(C) Eight-week-old WT mice were infected with 2.5×10^4 PFU of ZIKV intravaginally. Vaginal washes were collected at 6 hr and 24 hr post-infection and viral load was analyzed by RT-qPCR. (*$p < 0.05$).

(D and E) WT mice were infected with 1.5×10^5 PFU of ZIKV intraperitoneally (ip) or ivag and harvested on 1 and 3 dpi. RNA was isolated from the spleen (D) and vagina (E), and ZIKV levels were analyzed by RT-qPCR and normalized to *Hprt*.

(F and G) On 2 dpi (F), and 5 dpi (G), ZIKV levels in whole blood from mice in (A and B) were analyzed by RT-qPCR. ZIKV levels from the blood are normalized to *Hprt*.

For (A, B, F, G), results shown are mean ± SEM involving uninfected (n = 7), WT (n = 9), *Mx1* (n = 5), *Rag2*$^{-/-}$ (n = 8), *Ifnar1*$^{-/-}$ (n = 7), *Tlr7*$^{-/-}$ *Mavs*$^{-/-}$*Mx1* (n = 9), and *Irf3*$^{-/-}$ *Irf7*$^{-/-}$ (n = 4) mice pooled from two independent replicates. For (C), individual values from (n = 5) WT mice collected at indicated time points are shown. For (D, E), results shown are mean ± SEM involving uninfected (n = 4-5), IP infected (n = 6), ivag infected (n = 6) per time point pooled from two independent replicates. The gray dashed line represents the limit of detection. See also Figure S1 and Table S1.

No viral RNA was detected within the vagina following intraperitoneal injection (Figure 1E). Our results show that the female reproductive tract supports productive ZIKV replication even in WT mice, and this route of transmission supports persistent and higher levels of viral replication compared to after intraperitoneal infection.

RNA Sensors, Signaling and Type I Interferons Control Vaginal ZIKV Replication

Next, we examined the ability of innate and adaptive immune responses to control ZIKV replication in the vagina. Recombination activating gene-2-deficient (*Rag2*$^{-/-}$) mice, which lack T and B cells, harbored similar levels of ZIKV in the vagina as WT mice (Figures 1A, S1C), indicating that early viral replication in the vagina is not controlled by adaptive immune responses. We thus focused on innate mechanisms of ZIKV control. First, we examined the role of IFNAR in ZIKV control. Virgin female *Ifnar1*$^{-/-}$ mice challenged with ZIKV vaginally all harbored high levels of local ZIKV replication starting on 2 dpi, and ZIKV continued to replicate in the vaginal tissue of these mice through 7 dpi (Figures 1A, S1C). These results indicate that type I IFNs play a critical role in blocking ZIKV replication in the vaginal

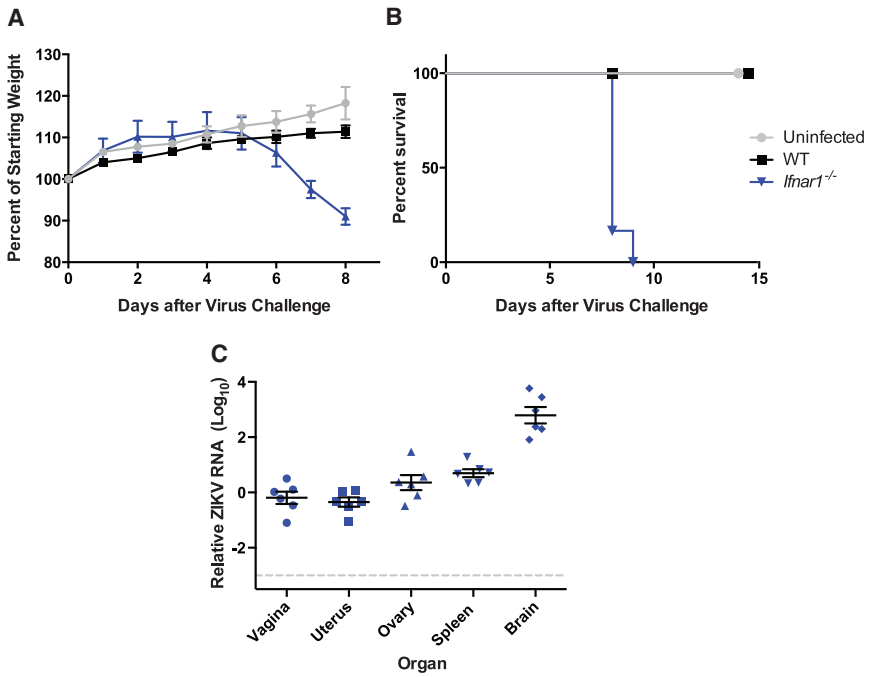

Figure 2. Vaginal Infection with High Doses of ZIKV Is Lethal in IFNAR-Deficient Mice

(A–C) Four- to 5-week-old Depo-Provera-treated virgin female mice of the indicated genotypes were infected intravaginally with 5.2×10^5 PFU of ZIKV. Mice were monitored for weight loss until 8 dpi (A) and survival until 14 dpi (B). All *Ifnar1*$^{-/-}$ mice developed hind limb paralysis and were euthanized after developing hind limb paralysis. Graphs are pooled from 2 independent replicates involving uninfected (n = 4), WT (n = 6), and *Ifnar1*$^{-/-}$(n = 6) mice. (C) Organs of euthanized *Ifnar1*$^{-/-}$ mice were harvested and levels of ZIKV RNA was analyzed by RT-pPCR. Results shown are mean ± standard error of the mean. Bars represent the mean of six *Ifnar1*$^{-/-}$ mice. The gray dashed line represents limit of detection.

mucosa. Given the importance of type I IFNs, we next examined the role of a well-known ISG, myxovirus resistance protein 1 (*Mx1*) in control of ZIKV in the vaginal mucosa. C57BL/6 mice carry nonfunctional alleles of the *Mx1* gene, a dynamin-like GTPase that blocks a wide range of RNA viruses (Haller et al., 2015). Yet, *Mx1* congenic mice on C56BL/6 background were no more capable of controlling ZIKV than the *Mx1*-deficient C57BL/6 mice (Figures 1A, S1C), indicating that Mx1 is not a relevant ISG that restricts ZIKV.

Next, we examined the role of RNA sensors that are known to trigger IFN induction in ZIKV control. We used mice deficient in *Tlr7*, *Mavs*, or both. *Mx1* congenic mice with single deletion in *Tlr7* harbored vaginal ZIKV titers comparable to the WT counterpart, whereas all *Mavs*-deficient mice had elevated viral titers at all time points compared to WT *Mx1* mice (Figure S1D). In contrast, mice deficient in both *Tlr7* and *Mavs* supported more than an order of magnitude higher titers of ZIKV in the vaginal mucosa than the WT mice (Figure 1A and Figure S1D), indicating redundancy between TLR7 and RLRs in ZIKV control. In contrast, mice deficient in cGAS had vaginal ZIKV titers comparable to WT mice (Figure S1C), indicating that this sensor is dispensable for ZIKV control in this tissue. TLR7 and RLRs utilize IRF3 and IRF7 for signaling for type I IFN synthesis (Honda and Taniguchi, 2006; Honda et al., 2005). Consistently, mice deficient in both IRF3 and IRF7 harbored high titers of local ZIKV replication starting on 2 dpi, reaching peak titers on 4–5 dpi, and continue to persist until 7 dpi (Figures 1A, S1C). All mice, except for one of seven *Ifnar1*$^{-/-}$ mice, survived after vaginal infection with 2.5×10^4 PFU of ZIKV with no signs of weight loss (Figure 1B). Of note, *Ifnar1*$^{-/-}$ mice had the highest levels of viremia 2 dpi (Figure 1F). Levels of viremia increased by 5 dpi in *Ifnar1*$^{-/-}$ mice and in *Irf3*$^{-/-}$ *Irf7*$^{-/-}$ mice (Figure 1G). These results indicated that IFNAR signaling is essential in preventing systemic ZIKV spread following vaginal replication.

High-Dose Vaginal ZIKV Challenge Is Lethal in IFNAR-Deficient Mice

Even at a higher dose (5.2×10^5 PFU) of vaginal ZIKV challenge, infected WT mice did not lose weight (Figure 2A) and all survived (Figure 2B). However, when *Ifnar1*$^{-/-}$ mice were challenged with a higher dose (5.2×10^5 PFU) of ZIKV, all mice began to lose weight by 6 dpi and died by 9 dpi (Figures 2A and 2B). Similar to reports of subcutaneous or intravenous infection (Dowall et al., 2016; Lazear et al., 2016; Rossi et al., 2016), all *Ifnar1*$^{-/-}$ mice developed hind limb paralysis. At the time of euthanasia, *Ifnar1*$^{-/-}$ mice had ZIKV RNA in the vagina, uterus, and ovaries as well as systemically in the spleen and brain (Figure 2C). In the absence of IFNAR, vaginal infection of ZIKV led to central nervous system (CNS) infection and death, demonstrating that vaginal infection by ZIKV spread systemically if the host innate immune response is compromised, leading to lethal disease.

Vaginal Infection of Dams Early During Pregnancy Results in Reduced Fetal Weight

Based on our finding that ZIKV replicates well in the vaginal mucosa of virgin mice (Figures 1 and S1), we hypothesized that ZIKV infection of pregnant mothers might have negative consequences on fetal development. To test this hypothesis, we infected pregnant WT dams at two early phases of pregnancy, at embryonic days 4.5 (E4.5) or E8.5. In mice, E4.5 corresponds to the initiation of embryonic development at the late blastocyst stage, whereas E8.5 corresponds to late gastrulation and the beginning of organogenesis (Ko, 2001). ZIKV replicated substantially in the vaginal tract after vaginal exposure of WT pregnant dams at E4.5 and at E8.5 (Figure 3A). These data indicated that even in the absence of Depo-Provera injection, WT mice are susceptible to vaginal viral replication during pregnancy.

Next, we examined the ZIKV infection of the maternal and fetal tissues. In WT mice we did not detect any ZIKV RNA

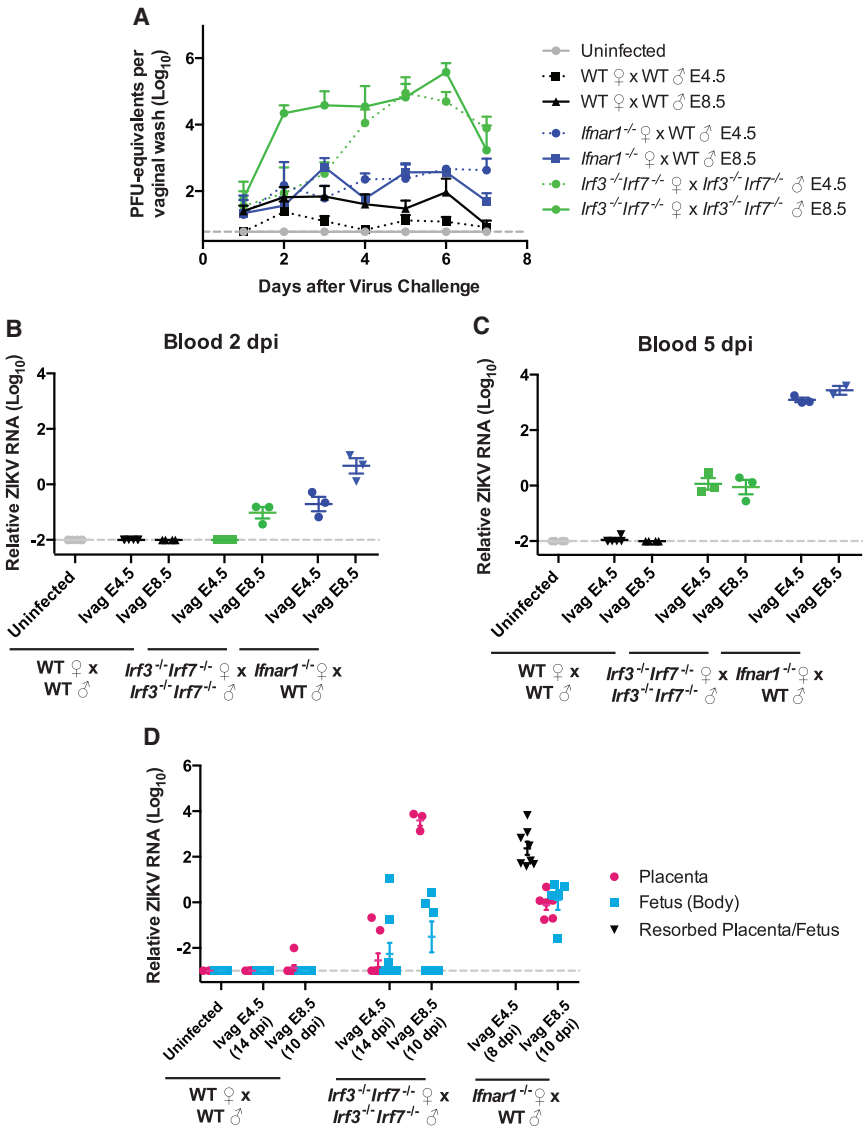

Figure 3. ZIKV Replicates in the Vaginal Mucosa of Pregnant Mice and Infects the Placenta in Mice Lacking the IFN Pathway

(A) Mice of indicated genotypes were infected intravaginally on E4.5 or E8.5 with 1.5×10^5 PFU of Cambodian ZIKV. On the indicated days post-infection, vaginal washes were collected and viral load was analyzed by RT-qPCR.

(B and C) On 2 dpi (B), and 5 dpi (C), ZIKV levels in whole blood were analyzed by RT-qPCR. ZIKV RNA from the blood are normalized to *Hprt*.

(D) On E18.5, placenta and fetal bodies were analyzed for presence of ZIKV using RT-pPCR. ZIKV RNA was normalized to *Hprt*. Resorbed fetuses from *Ifnar1*$^{-/-}$ dams infected E4.5 were harvested on E12.5.

For (A–C) results shown are the mean ± SEM involving uninfected (n = 4), WT E4.5 (n = 6), WT E8.5 (n = 5), *Irf3*$^{-/-}$ *Irf7*$^{-/-}$ E4.5 (n = 3), *Irf3*$^{-/-}$ *Irf7*$^{-/-}$ E8.5 (n = 3), *Ifnar1*$^{-/-}$ E4.5 (n = 3), and *Ifnar1*$^{-/-}$ E8.5 (n = 3) pregnant dams. For (D), 2–4 pregnant dams per group were infected, and n = 3-8 placentas or fetuses were analyzed. The gray dashed line represents limit of detection.

Deficiencies in the Interferon Pathways Exacerbate Fetal Growth Restriction following Vaginal ZIKV Infection of Dams

Having established IUGR in WT mice following vaginal ZIKV exposure during early phases of pregnancy, we next investigated the role of PRR and IFNAR signaling in controlling ZIKV replication in the mother and fetus. To this end, *Irf3*$^{-/-}$*Irf7*$^{-/-}$ dams mated with *Irf3*$^{-/-}$*Irf7*$^{-/-}$ sires or *Ifnar1*$^{-/-}$ dams mated with WT sires (Miner et al., 2016), were challenged intravaginally with ZIKV on E4.5 or E8.5. Consistent with what was seen in virgin females, in *Ifnar1*$^{-/-}$ dams, ZIKV replication in the vagina was increased compared to WT mice, and we detected significant levels of ZIKV in maternal blood at 2 dpi, which was elevated on 5 dpi (Figures 3A–3C). In *Irf3*$^{-/-}$ *Irf7*$^{-/-}$ dams, consistent with what was seen with virgin females, replication in the vagina was even higher than for *Ifnar1*$^{-/-}$ mice (Figure 3A). Infection at E8.5 but not E4.5 resulted in detectable viremia on 2 dpi, and viremia was elevated in both conditions by 5 dpi (Figures 3B and 3C). We detected high levels of ZIKV RNA in the placenta and fetal bodies of *Irf3*$^{-/-}$ *Irf7*$^{-/-}$ mice infected at E8.5 (10 dpi) (Figure 3D). In addition, ZIKV RNA was detected in some of the placentas and the bodies of *Irf3*$^{-/-}$ *Irf7*$^{-/-}$ fetuses infected on E4.5 (14 dpi) (Figure 3D). There were also high levels of ZIKV RNA detected in the placenta and body of the fetuses of *Ifnar1*$^{-/-}$ dams infected on E8.5 (10 dpi) and of the resorbed fetuses of *Ifnar1*$^{-/-}$ dams infected at E4.5 (14 dpi) (Figure 3D). Interestingly, ZIKV RNA levels were several orders of magnitude higher in the placentas of *Irf3*$^{-/-}$ *Irf7*$^{-/-}$ dams compared to those in the peripheral blood on 2 or 5 dpi (Figures 3B and 3C). Further at E18.5 (just prior to birth), we detected no virus in the placenta or fetal bodies in neither the E4.5 nor E8.5 infection time points (Figure 3D). However, these data do not rule out the possibility that ZIKV infection of the placenta and fetus occurred earlier, between days 1–10 (E8.5) or days 1–14 (E4.5) of viral challenge. Despite our inability to detect ZIKV RNA by qPCR in the maternal blood, fetal body, or placenta, when pregnant WT dams were infected on E4.5, the developing embryo at E18.5 had mild but significant overall growth defect (Figure 4A). In contrast, when WT dams were infected on E8.5, the weight of the fetuses was comparable to those of uninfected controls when analyzed at E18.5 (Figure 4A). These data indicated that ZIKV replicates in the vagina of WT pregnant dams and has a negative impact on fetal growth when the viral exposure occurs during early pregnancy.

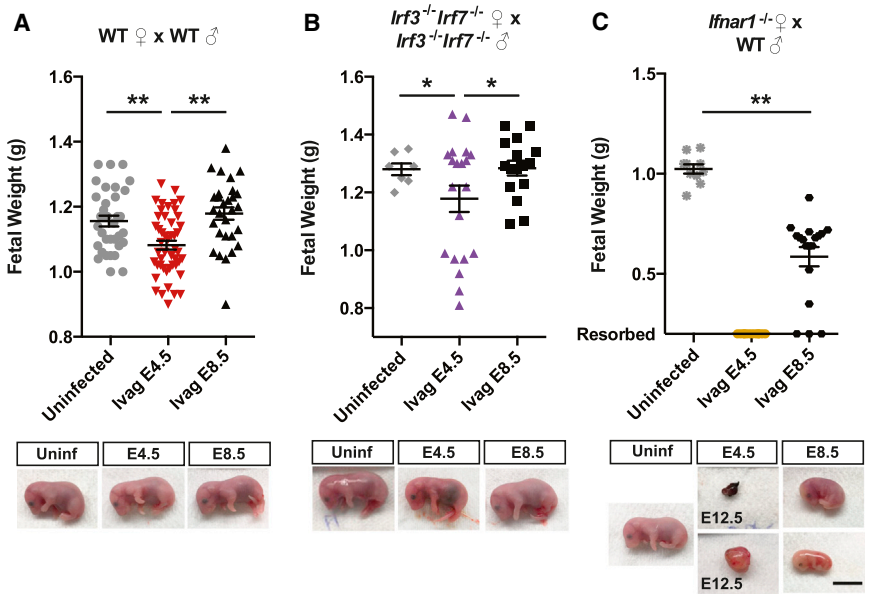

Figure 4. Vaginal Infection of Pregnant Female Mice Leads to Fetal Growth Impairment and Fetal Resorption

(A–C) Mice of indicated genotypes were infected intravaginally on E4.5 or E8.5 with 1.5 × 10^5 PFU of Cambodian ZIKV intravaginally. On E18.5, fetal weight was measured. Representative pictures of fetuses from each indicated genotype and day of infection are shown. All were harvested at E18.5 unless otherwise indicated. (**p = < 0.001, *p = < 0.05, scale bar, 1cm). For the *Ifnar1*$^{-/-}$ dams mated with WT sire infected on E4.5, the upper panel shows the dissected aborted fetus, and the lower panel shows the entire fetal sac. Upper panel bars indicate the mean ± SEM of the weights of 7–34 pups from 1–4 pregnant dams per genotype for uninfected mice and 16–48 pups from 2–6 pregnant dams per genotype per time point infected.

of the *Ifnar1*$^{-/-}$ dams (Figure 3D). These results indicate that vaginal exposure of ZIKV results in higher levels of viral replication in the vaginal mucosa in the absence of IRF3/IRF7 or IFNAR in pregnant mice. Subsequently, the virus enters the blood stream and infects the placenta and fetal bodies.

While no impact on fetal weight was observed after infection of *Irf3*$^{-/-}$ *Irf7*$^{-/-}$ dams on E8.5 (Figure 4B), fetal weight was significantly reduced in *Irf3*$^{-/-}$ *Irf7*$^{-/-}$ dams infected on E4.5, albeit variable (Figure 4B). In *Ifnar1*$^{-/-}$ dams mated to WT sires, ivag infection on E4.5 led to resorption of all fetuses, which are all *Ifnar1*$^{+/-}$, by 8 dpi (Figure 4C). After infection on E8.5, fetuses from *Ifnar1*$^{-/-}$ × WT parents survived until E18.5, but they showed significantly reduced fetal weight at E18.5 compared to the uninfected controls (Figure 4C). Therefore, IFNAR expression and autonomous fetal immune defense are insufficient to protect against ZIKV infection, akin to the results found after subcutaneous ZIKV challenge (Miner et al., 2016).

Vaginal Infection Results in Fetal Brain Infection in WT Mice

While we observed significant IUGR in fetuses of pregnant dams infected on E4.5, we did not detect ZIKV RNA in the fetal body (Figure 3D) or fetal brain (data not shown) at E18.5 in infected WT mice. Although we were unable to detect ZIKV RNA in the brain at E18.5, previous studies suggest that fetal brain infection of WT mice occurs only in specific cell subsets and regions of the brain (Wu et al., 2016), likely limiting the sensitivity of RT-qPCR (Miner et al., 2016). Therefore, we decided to further examine the presence of ZIKV in fetal brains by immuno-electron microscopy (EM) using an antibody specific to flavivirus NS1.

Strikingly, a number of ZIKV-infected cells were detected in the E18.5 cortex (Figures 5A and 5D) and cerebellum (Figures 5B, 5C, 5E, and 5F) of brains isolated from WT fetuses whose mothers were vaginally infected on E4.5 or on E8.5. Virions were readily detected in these cells (see arrows). Further, the immuno-EM images show clear immunoreactivity for NS1, which was expressed abundantly in the ER of the infected cells found in the cerebellum and the cortex (Figures 5C and 5E, see arrowheads). The NS1 labeling is consistent with the fact that NS1 of flaviviruses is inserted into the lumen of the ER (Chambers et al., 1990). None of the uninfected mice contained virions or NS1 labeling in any regions of the brain tested (data not shown). Both neurons (Figures 5A–5D) and glial cells (Figure 5E) were infected with ZIKV. Further, we found evidence of virus within the endothelial cells, as well as NS1 staining on the luminal side of the endothelial cells (Figure 5F). These results suggest production of ZIKV in nearby tissues, as it is known that flavivirus NS1 is also abundantly secreted by infected cells in a multimeric form (Crooks et al., 1994; Flamand et al., 1999). Therefore, these results demonstrate that despite grossly normal fetal size (Figure 4), vaginal infection of WT mothers with ZIKV results in viral invasion of the fetal brain tissue and causes significant levels of infection in the fetus of WT mice.

DISCUSSION

In this study, we demonstrate that vaginal ZIKV infection of female mice leads to productive replication of the virus within the vaginal mucosa even in WT animals. This was observed in both virgin female mice that were pretreated with Depo-Provera and in pregnant dams. Direct comparison of ZIKV RNA in the spleen after intraperitoneal injection and in the vagina after intravaginal inoculation revealed that the vaginal mucosa supports robust viral replication compared to other organs. In pregnant WT mice, ZIKV replication in the vaginal tissue was followed by the infection of fetal brain and IUGR, despite the absence of viremia. These results highlight the vaginal tract as a susceptible site for ZIKV replication, even in immunocompetent hosts. The consequences of vaginally-acquired ZIKV infection on the fetus appear to vary depending on the gestation stage at which the virus was introduced. Vaginal ZIKV exposure at early pregnancy (E4.5) resulted in IUGR of the fetus, while exposure at E8.5

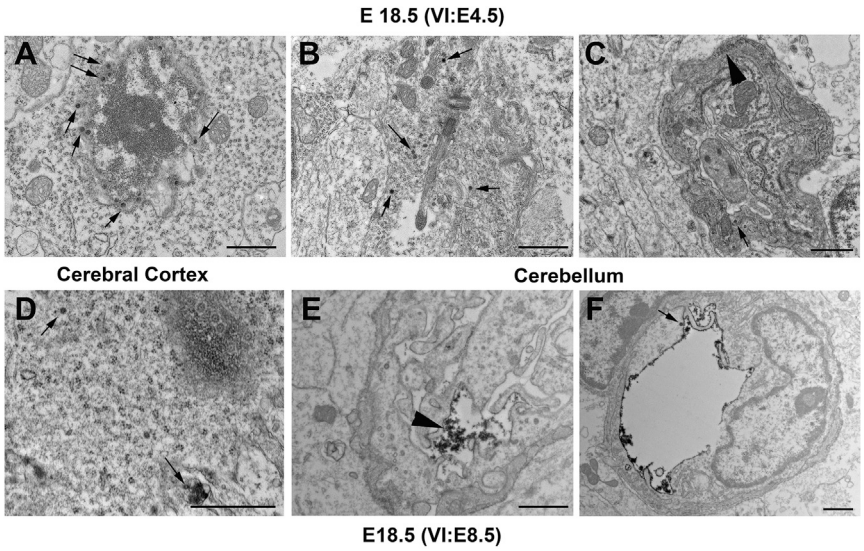

Figure 5. Vaginal Infection of Pregnant Female WT Mice Leads to Fetal Brain Infection

(A–F) Immuno-EM depicting ZIKV infected cells (anti-flavivirus NS1 antibody) in the cortex (A and D) and cerebellum (B, C, E, and F) of WT fetal brain from WT dams infected at E4.5 (A–C) and E8.5 (D–F) sacrificed on E18.5. Arrows indicate the ZIKV virions within the infected cells. Arrowheads indicate immunolabeling of NS1. The cells depicted in are neurons (A–D), glial cell (E), and endothelial cells (F). Scale bar, 1 μm in all panels. These figures are representative of 2–4 brains examined for each group.

resulted in normal fetal weight. Nevertheless, ZIKV-infected cells were found within the cerebellum and the cortex of the fetal brain after infection at both time points. Therefore, the female genital tract represents a productive site of viral replication. Our studies also indicate that ZIKV brain infection can occur in fetuses without causing gross growth defects or malformations. It will be important to further investigate how fetal brain infection with ZIKV impacts the postnatal brain development and the cognitive functions of the offspring.

By using the vaginal ZIKV infection model, we also interrogated the components of the protective immune responses. Deficiencies in *Tlr7* led to no increase in viral titers over WT counterpart, while deletion of the *Mavs* gene resulted in slightly elevated ZIKV titers, indicating a more essential role of RLR signaling in ZIKV control. However, deficiencies in both *Tlr7* and *Mavs* resulted in more than an order of magnitude higher titers of ZIKV in the vaginal mucosa, placing TLR7 and RLRs as redundant key upstream sensors that control ZIKV replication. While cGAS is important in controlling West Nile virus infection (Schoggins et al., 2014), we found no differences in ZIKV replication following vaginal exposure. In addition, our studies showed that transcription factors IRF3 and IRF7 are required to block local ZIKV replication. Further, IFNAR is critical for preventing both local viral replication and systemic spread of the virus. In contrast, adaptive immunity plays a minimal role in controlling vaginal ZIKV infection during the early phase of infection.

PRR signaling stimulates the activation of IRF3 and IRF7, which bind to their respective IRF binding element (IRFE) to turn on both type I IFN genes as well as ISGs. Once secreted, type I IFNs bind to the cell-surface receptor, IFNAR, inducing activation of receptor-associated Jak kinases, followed by recruitment and phosphorylation of STAT1 and STAT2. STAT1, STAT2, and IFN regulatory factor 9 (IRF9) form a trimeric transcription factor complex, known as IFN stimulated gene factor 3 (ISGF3), which binds to IFN-stimulated response elements (ISREs) in ISG promoters. Due to the high degree of homology between the ISRE and IRFE consensus sequences, the transcription of many ISGs can be directly induced by either ISGF3, IRF3 or IRF7 (Schmid et al., 2010). Comparing our results from *Irf3*$^{-/-}$ *Irf7*$^{-/-}$ mice (which lack IRFE-inducible ISGs downstream of PRR signaling) and *Ifnar1*$^{-/-}$ mice (which lack ISRE-inducible ISGs) informs us that PRR-signal-induced ISGs are more critical in controlling ZIKV replication in the vagina and placenta, while IFNAR-induced ISGs are more important in blocking systemic spread of the virus from the vagina to the blood stream. Our data suggest that there must be some levels of type I IFN secreted to limit systemic viral spread in the infected *Irf3*$^{-/-}$ *Irf7*$^{-/-}$ mice. This is consistent with previous studies showing that mice lacking IRF3 and IRF7 have an intact IFN-β responses to West Nile virus (Daffis et al., 2009; Lazear et al., 2013). Further, our data suggest the presence of additional PRRs in conferring resistance, as *Tlr7*$^{-/-}$ *Mavs*$^{-/-}$ mice harbored less ZIKV in the vaginal mucosa compared to the *Irf3*$^{-/-}$ *Irf7*$^{-/-}$ mice (Figure 1A). Conversely, given the higher levels of viral burden in the *Irf3*$^{-/-}$ *Irf7*$^{-/-}$ mice compared to the *Ifnar1*$^{-/-}$ mice, we conclude that type I IFN-independent, PRR-dependent ISGs in the vagina and placenta are able to further block local viral replication. We ruled out *Mx1* as such an ISG. Furthermore, our studies illustrate that different components of the innate immune response are responsible for controlling the degree of local viral replication in the exposed tissue and systemic spread of viruses and provide a model to further dissect these components. Future studies are needed to dissect the exact cell types and genes involved in controlling sexually transmitted ZIKV in the female reproductive tract.

Vaginal exposure of ZIKV in pregnant mice resulted in IUGR and fetal brain infection in the absence of viremia in WT mice. These data suggest a possible direct transmission route from the vaginal tract through the cervix to the intrauterine space. From there, the virus may enter the decidua and infect the placenta, thereby entering the fetus through the umbilical cord. Alternatively, the virus may spread from the decidua to invade the chorion and amnion and enter the amniotic cavity to directly infect the fetus. Because of the absence of viremia in infected WT dams, we hypothesize that the vaginal transmission of ZIKV might give the virus a direct access to the placenta or the fetus via an ascending route. Our studies also highlight that, even though WT mice are able to control ZIKV well compared to mice lacking IFNAR signaling, the virus still has a high

predilection for the developing fetal brain. Consistent with a previous study (Wu et al., 2016), our study shows that infection of the fetal brain of WT C57BL/6 does occur when pregnant dams are infected with ZIKV.

Vaginal ZIKV exposure of dams deficient in IRF3 and IRF7 resulted in very high levels of viral replication in the vaginal tissue. In contrast to WT mice, some of these *Irf3*$^{-/-}$ *Irf7*$^{-/-}$ mice also supported ZIKV replication in the placenta and fetal bodies. Further, IFNAR-deficient dams infected with ZIKV early during pregnancy led to fetal loss and later during pregnancy led to severe IUGR. Because both of these genotypes support viremia, ZIKV may infect the placenta through blood-placental transmission and bypass the placental barrier to infect the fetus. These results are consistent with the hematogenous transplacental route of infection described by Miner et al. (Miner et al., 2016), who showed viremia and IUGR following subcutaneous infection of *Ifnar1*$^{-/-}$ dams at E6.5 or E7.5.

How might our findings apply to humans? A recent study demonstrated that ZIKV NS5 protein antagonizes human STAT2 but not mouse STAT2 (Grant et al., 2016). Therefore, humans are naturally more susceptible to ZIKV infection than mice because infected cells can no longer respond to IFNs. Consequently, we speculate that ZIKV introduced into the human vagina is likely to replicate more robustly than in the vaginal cavity of WT mice. Our findings that ZIKV replicates in the vagina of mice is consistent with the report of sexual transmission from an infected female to her uninfected male partner. Currently, we do not know if sexual transmission of ZIKV poses a different risk of birth defects than mosquito-borne transmission in pregnant women. However, our results from the mouse model would predict negative consequences on fetal development following vaginal ZIKV exposure of the mothers during early pregnancy. Finally, while mosquito-borne transmission is blamed for the increased incidence of microcephaly, it is possible that sexual transmission of ZIKV might account for some of the fetal diseases even within the *Aedes* ZIKV endemic regions. Given the fact that human placental trophoblasts provide protective type III IFNs (Bayer et al., 2016), ascending infection from the vagina to the fetus in humans may provide the ZIKV direct access. Our findings in mice indicate that sexual transmission of ZIKV is harmful to the fetus and provide a model to study the impact of interventional and therapeutic treatment of vaginal ZIKV viral infection during pregnancy.

STAR★METHODS

Detailed methods are provided in the online version of this paper and include the following:

- KEY RESOURCES TABLE
- CONTACT FOR REAGENTS AND RESOURCE SHARING
- EXPERIMENTAL MODEL AND SUBJECT DETAILS
  - Mice
  - Viruses
- METHOD DETAILS
  - In Vivo Infections
  - Quantification of ZIKV Genome by qRT-PCR
  - Quantification of ZIKV by Plaque Assay
  - Electron Microscopy
- QUANTIFICATION AND STATISTICAL ANALYSIS
  - Data Analysis

SUPPLEMENTAL INFORMATION

Supplemental Information includes one figure and one table and can be found with this article online at http://dx.doi.org/10.1016/j.cell.2016.08.004.

AUTHOR CONTRIBUTIONS

Conceptualization, L.J.Y., T.L.H., A.I.; Investigation, L.J.Y., W.K.-H., T.R., S.L.F., L.V., B.S., K.S-B.; Resources, B.D.L., A.V.d.P.; Writing, L.J.Y., A.I. Supervision, T.L.H., A.I.; Funding Acquisition, A.I.

ACKNOWLEDGMENTS

We thank Huiping Dong for technical support and the members of the Erol Fikrig laboratory for helpful discussions. We thank Dr. Marie Flamand at the Institut Pasteur in Paris for providing us the antibody to NS1. This work was supported by the Howard Hughes Medical Institute, and National Institutes of Health (NIH) grants R01 AI054359 (A.I.). L.J.Y. is supported by NIH Medical Scientist Training Program Training Grant T32 GM007205. S.L.F. is supported by K08 AI119142.

Received: July 3, 2016
Revised: July 29, 2016
Accepted: August 3, 2016
Published: August 25, 2016

REFERENCES

Bayer, A., Lennemann, N.J., Ouyang, Y., Bramley, J.C., Morosky, S., Marques, E.T., Jr., Cherry, S., Sadovsky, Y., and Coyne, C.B. (2016). Type III Interferons Produced by Human Placental Trophoblasts Confer Protection against Zika Virus Infection. Cell Host Microbe *19*, 705–712.

Bruni, D., Chazal, M., Sinigaglia, L., Chauveau, L., Schwartz, O., Desprès, P., and Jouvenet, N. (2015). Viral entry route determines how human plasmacytoid dendritic cells produce type I interferons. Sci. Signal. *8*, ra25.

Chambers, T.J., Hahn, C.S., Galler, R., and Rice, C.M. (1990). Flavivirus genome organization, expression, and replication. Annu. Rev. Microbiol. *44*, 649–688.

Crooks, A.J., Lee, J.M., Easterbrook, L.M., Timofeev, A.V., and Stephenson, J.R. (1994). The NS1 protein of tick-borne encephalitis virus forms multimeric species upon secretion from the host cell. J. Gen. Virol. *75*, 3453–3460.

Cugola, F.R., Fernandes, I.R., Russo, F.B., Freitas, B.C., Dias, J.L., Guimarães, K.P., Benazzato, C., Almeida, N., Pignatari, G.C., Romero, S., et al. (2016). The Brazilian Zika virus strain causes birth defects in experimental models. Nature *534*, 267–271.

Daffis, S., Suthar, M.S., Szretter, K.J., Gale, M., Jr., and Diamond, M.S. (2009). Induction of IFN-beta and the innate antiviral response in myeloid cells occurs through an IPS-1-dependent signal that does not require IRF-3 and IRF-7. PLoS Pathog. *5*, e1000607.

Davidson, A., Slavinski, S., Komoto, K., Rakeman, J., and Weiss, D. (2016). Suspected Female-to-Male Sexual Transmission of Zika Virus - New York City, 2016. MMWR Morb. Mortal. wkly. Rep. *65*, 716–717.

Décembre, E., Assil, S., Hillaire, M.L., Dejnirattisai, W., Mongkolsapaya, J., Screaton, G.R., Davidson, A.D., and Dreux, M. (2014). Sensing of immature particles produced by dengue virus infected cells induces an antiviral response by plasmacytoid dendritic cells. PLoS Pathog. *10*, e1004434.

Deckard, D.T., Chung, W.M., Brooks, J.T., Smith, J.C., Woldai, S., Hennessey, M., Kwit, N., and Mead, P. (2016). Male-to-Male Sexual Transmission of Zika Virus - Texas, January 2016. MMWR Morb. Mortal. wkly. Rep. *65*, 372–374.

Dowall, S.D., Graham, V.A., Rayner, E., Atkinson, B., Hall, G., Watson, R.J., Bosworth, A., Bonney, L.C., Kitchen, S., and Hewson, R. (2016). A Susceptible Mouse Model for Zika Virus Infection. PLoS Negl. Trop. Dis. *10*, e0004658.

Driggers, R.W., Ho, C.Y., Korhonen, E.M., Kuivanen, S., Jääskeläinen, A.J., Smura, T., Rosenberg, A., Hill, D.A., DeBiasi, R.L., Vezina, G., et al. (2016). Zika Virus Infection with Prolonged Maternal Viremia and Fetal Brain Abnormalities. N. Engl. J. Med. *374*, 2142–2151.

Flamand, M., Megret, F., Mathieu, M., Lepault, J., Rey, F.A., and Deubel, V. (1999). Dengue virus type 1 nonstructural glycoprotein NS1 is secreted from mammalian cells as a soluble hexamer in a glycosylation-dependent fashion. J. Virol. *73*, 6104–6110.

Foxman, E.F., Storer, J.A., Fitzgerald, M.E., Wasik, B.R., Hou, L., Zhao, H., Turner, P.E., Pyle, A.M., and Iwasaki, A. (2015). Temperature-dependent innate defense against the common cold virus limits viral replication at warm temperature in mouse airway cells. Proc. Natl. Acad. Sci. USA *112*, 827–832.

Foy, E., Li, K., Sumpter, R., Jr., Loo, Y.M., Johnson, C.L., Wang, C., Fish, P.M., Yoneyama, M., Fujita, T., Lemon, S.M., and Gale, M., Jr. (2005). Control of antiviral defenses through hepatitis C virus disruption of retinoic acid-inducible gene-I signaling. Proc. Natl. Acad. Sci. USA *102*, 2986–2991.

Foy, B.D., Kobylinski, K.C., Chilson Foy, J.L., Blitvich, B.J., Travassos da Rosa, A., Haddow, A.D., Lanciotti, R.S., and Tesh, R.B. (2011). Probable non-vector-borne transmission of Zika virus, Colorado, USA. Emerg. Infect. Dis. *17*, 880–882.

Grant, A., Ponia, S.S., Tripathi, S., Balasubramaniam, V., Miorin, L., Sourisseau, M., Schwarz, M.C., Sánchez-Seco, M.P., Evans, M.J., Best, S.M., and García-Sastre, A. (2016). Zika Virus Targets Human STAT2 to Inhibit Type I Interferon Signaling. Cell Host Microbe *19*, 882–890.

Haddow, A.D., Schuh, A.J., Yasuda, C.Y., Kasper, M.R., Heang, V., Huy, R., Guzman, H., Tesh, R.B., and Weaver, S.C. (2012). Genetic characterization of Zika virus strains: geographic expansion of the Asian lineage. PLoS Negl. Trop. Dis. *6*, e1477.

Haller, O., Staeheli, P., Schwemmle, M., and Kochs, G. (2015). Mx GTPases: dynamin-like antiviral machines of innate immunity. Trends Microbiol. *23*, 154–163.

Hills, S.L., Russell, K., Hennessey, M., Williams, C., Oster, A.M., Fischer, M., and Mead, P. (2016). Transmission of Zika Virus Through Sexual Contact with Travelers to Areas of Ongoing Transmission - Continental United States, 2016. MMWR Morb. Mortal. wkly. Rep. *65*, 215–216.

Honda, K., and Taniguchi, T. (2006). IRFs: master regulators of signalling by Toll-like receptors and cytosolic pattern-recognition receptors. Nat. Rev. Immunol. *6*, 644–658.

Honda, K., Yanai, H., Negishi, H., Asagiri, M., Sato, M., Mizutani, T., Shimada, N., Ohba, Y., Takaoka, A., Yoshida, N., and Taniguchi, T. (2005). IRF-7 is the master regulator of type-I interferon-dependent immune responses. Nature *434*, 772–777.

Honda, K., Takaoka, A., and Taniguchi, T. (2006). Type I interferon [corrected] gene induction by the interferon regulatory factor family of transcription factors. Immunity *25*, 349–360.

Janeway, C.A., Jr. (1989). Approaching the asymptote? Evolution and revolution in immunology. Cold Spring Harb. Symp. Quant. Biol. *54*, 1–13.

Ko, M.S. (2001). Embryogenomics: developmental biology meets genomics. Trends Biotechnol. *19*, 511–518.

Lanciotti, R.S., Kosoy, O.L., Laven, J.J., Velez, J.O., Lambert, A.J., Johnson, A.J., Stanfield, S.M., and Duffy, M.R. (2008). Genetic and serologic properties of Zika virus associated with an epidemic, Yap State, Micronesia, 2007. Emerg. Infect. Dis. *14*, 1232–1239.

Lazear, H.M., and Diamond, M.S. (2016). Zika Virus: New Clinical Syndromes and Its Emergence in the Western Hemisphere. J. Virol. *90*, 4864–4875.

Lazear, H.M., Lancaster, A., Wilkins, C., Suthar, M.S., Huang, A., Vick, S.C., Clepper, L., Thackray, L., Brassil, M.M., Virgin, H.W., et al. (2013). IRF-3, IRF-5, and IRF-7 coordinately regulate the type I IFN response in myeloid dendritic cells downstream of MAVS signaling. PLoS Pathog. *9*, e1003118.

Lazear, H.M., Govero, J., Smith, A.M., Platt, D.J., Fernandez, E., Miner, J.J., and Diamond, M.S. (2016). A Mouse Model of Zika Virus Pathogenesis. Cell Host Microbe *19*, 720–730.

Loo, Y.M., Fornek, J., Crochet, N., Bajwa, G., Perwitasari, O., Martinez-Sobrido, L., Akira, S., Gill, M.A., García-Sastre, A., Katze, M.G., and Gale, M., Jr. (2008). Distinct RIG-I and MDA5 signaling by RNA viruses in innate immunity. J. Virol. *82*, 335–345.

Mansuy, J.M., Dutertre, M., Mengelle, C., Fourcade, C., Marchou, B., Delobel, P., Izopet, J., and Martin-Blondel, G. (2016). Zika virus: high infectious viral load in semen, a new sexually transmitted pathogen? Lancet Infect. Dis. *16*, 405.

Martines, R.B., Bhatnagar, J., Keating, M.K., Silva-Flannery, L., Muehlenbachs, A., Gary, J., Goldsmith, C., Hale, G., Ritter, J., Rollin, D., et al. (2016). Notes from the Field: Evidence of Zika Virus Infection in Brain and Placental Tissues from Two Congenitally Infected Newborns and Two Fetal Losses–Brazil, 2015. MMWR Morb. Mortal. wkly. Rep. *65*, 159–160.

Medzhitov, R. (2001). Toll-like receptors and innate immunity. Nat. Rev. Immunol. *1*, 135–145.

Miner, J.J., Cao, B., Govero, J., Smith, A.M., Fernandez, E., Cabrera, O.H., Garber, C., Noll, M., Klein, R.S., Noguchi, K.K., et al. (2016). Zika Virus Infection during Pregnancy in Mice Causes Placental Damage and Fetal Demise. Cell *165*, 1081–1091.

Mlakar, J., Korva, M., Tul, N., Popović, M., Poljšak-Prijatelj, M., Mraz, J., Kolenc, M., Resman Rus, K., Vesnaver Vipotnik, T., Fabjan Vodušek, V., et al. (2016). Zika Virus Associated with Microcephaly. N. Engl. J. Med. *374*, 951–958.

Musso, D., Roche, C., Robin, E., Nhan, T., Teissier, A., and Cao-Lormeau, V.M. (2015). Potential sexual transmission of Zika virus. Emerg. Infect. Dis. *21*, 359–361.

Nazmi, A., Mukherjee, S., Kundu, K., Dutta, K., Mahadevan, A., Shankar, S.K., and Basu, A. (2014). TLR7 is a key regulator of innate immunity against Japanese encephalitis virus infection. Neurobiol. Dis. *69*, 235–247.

Parr, M.B., Kepple, L., McDermott, M.R., Drew, M.D., Bozzola, J.J., and Parr, E.L. (1994). A mouse model for studies of mucosal immunity to vaginal infection by herpes simplex virus type 2. Lab. Invest. *70*, 369–380.

Petersen, E.E., Polen, K.N., Meaney-Delman, D., Ellington, S.R., Oduyebo, T., Cohn, A., Oster, A.M., Russell, K., Kawwass, J.F., Karwowski, M.P., et al. (2016). Update: Interim Guidance for Health Care Providers Caring for Women of Reproductive Age with Possible Zika Virus Exposure–United States, 2016. MMWR Morb. Mortal. wkly. Rep. *65*, 315–322.

Pillai, P.S., Molony, R.D., Martinod, K., Dong, H., Pang, I.K., Tal, M.C., Solis, A.G., Bielecki, P., Mohanty, S., Trentalange, M., et al. (2016). Mx1 reveals innate pathways to antiviral resistance and lethal influenza disease. Science *352*, 463–466.

Prisant, N., Bujan, L., Benichou, H., Hayot, P.H., Pavili, L., Lurel, S., Herrmann, C., Janky, E., and Joguet, G. (2016). Zika virus in the female genital tract. Lancet Infect. Dis., S1473-3099(16)30193-1.

Rossi, S.L., Tesh, R.B., Azar, S.R., Muruato, A.E., Hanley, K.A., Auguste, A.J., Langsjoen, R.M., Paessler, S., Vasilakis, N., and Weaver, S.C. (2016). Characterization of a Novel Murine Model to Study Zika Virus. Am. J. Trop. Med. Hyg. *94*, 1362–1369.

Rowland, A., Washington, C.I., Sheffield, J.S., Pardo-Villamizar, C.A., and Segars, J.H. (2016). Zika virus infection in semen: a call to action and research. J. Assist. Reprod. Genet. *33*, 435–437.

Saito, T., Owen, D.M., Jiang, F., Marcotrigiano, J., and Gale, M., Jr. (2008). Innate immunity induced by composition-dependent RIG-I recognition of hepatitis C virus RNA. Nature *454*, 523–527.

Schmid, S., Mordstein, M., Kochs, G., García-Sastre, A., and Tenoever, B.R. (2010). Transcription factor redundancy ensures induction of the antiviral state. J. Biol. Chem. *285*, 42013–42022.

Schoggins, J.W., and Rice, C.M. (2011). Interferon-stimulated genes and their antiviral effector functions. Curr. Opin. Virol. *1*, 519–525.

Schoggins, J.W., MacDuff, D.A., Imanaka, N., Gainey, M.D., Shrestha, B., Eitson, J.L., Mar, K.B., Richardson, R.B., Ratushny, A.V., Litvak, V., et al. (2014). Pan-viral specificity of IFN-induced genes reveals new roles for cGAS in innate immunity. Nature *505*, 691–695.

Silasi, M., Cardenas, I., Kwon, J.Y., Racicot, K., Aldo, P., and Mor, G. (2015). Viral infections during pregnancy. Am. J. Reprod. Immunol. *73*, 199–213.

Takeuchi, O., and Akira, S. (2007). Recognition of viruses by innate immunity. Immunol. Rev. *220*, 214–224.

Town, T., Bai, F., Wang, T., Kaplan, A.T., Qian, F., Montgomery, R.R., Anderson, J.F., Flavell, R.A., and Fikrig, E. (2009). Toll-like receptor 7 mitigates lethal West Nile encephalitis via interleukin 23-dependent immune cell infiltration and homing. Immunity *30*, 242–253.

Venturi, G., Zammarchi, L., Fortuna, C., Remoli, M.E., Benedetti, E., Fiorentini, C., Trotta, M., Rizzo, C., Mantella, A., Rezza, G., and Bartoloni, A. (2016). An autochthonous case of Zika due to possible sexual transmission, Florence, Italy, 2014. Euro Surveill. *21* http://dx.doi.org/10.2807/1560-7917.ES.2016.21.8.30148.

Wang, J.P., Liu, P., Latz, E., Golenbock, D.T., Finberg, R.W., and Libraty, D.H. (2006). Flavivirus activation of plasmacytoid dendritic cells delineates key elements of TLR7 signaling beyond endosomal recognition. J. Immunol. *177*, 7114–7121.

Wang, L., Valderramos, S.G., Wu, A., Ouyang, S., Li, C., Brasil, P., Bonaldo, M., Coates, T., Nielsen-Saines, K., Jiang, T., et al. (2016). From Mosquitos to Humans: Genetic Evolution of Zika Virus. Cell Host Microbe *19*, 561–565.

Welte, T., Reagan, K., Fang, H., Machain-Williams, C., Zheng, X., Mendell, N., Chang, G.J., Wu, P., Blair, C.D., and Wang, T. (2009). Toll-like receptor 7-induced immune response to cutaneous West Nile virus infection. J. Gen. Virol. *90*, 2660–2668.

Wu, K.Y., Zuo, G.L., Li, X.F., Ye, Q., Deng, Y.Q., Huang, X.Y., Cao, W.C., Qin, C.F., and Luo, Z.G. (2016). Vertical transmission of Zika virus targeting the radial glial cells affects cortex development of offspring mice. Cell Res. *26*, 645–654.

STAR★METHODS

KEY RESOURCES TABLE

REAGENT or RESOURCE	SOURCE	IDENTIFIER
Antibodies		
Anti-NS1 antibody	Dr. Marie Flamand (PI)	17A12-1G5
biotinylated anti mouse secondary antibody	Vector	BA-2000
Chemicals, Peptides, and Recombinant Proteins		
Medroxyprogesterone acetate (Depo-Provera)	Pfizer	Cat#: NDC 0009-0626-01
ACM	Durcupan	EMS14040
amido black	MP Biochemicals	CAS - 1064-48-8 (02100563)
Critical Commercial Assays		
RNeasy Mini Kit	QIAGEN	Cat No./ID: 74106
Trizol	Thermo Fischer Scientific	15596026
iScript cDNA synthesis kit	Bio-Rad	1708891
PrimeTime master mix	Integrated DNA Technologies	1055772
Vectastain Elite ABC	Vector	PK-6100
Experimental Models: Cell Lines		
Vero	ATCC	ATCC: CCL81
C6/36 *Aedes albopictus* mosquito cells	ATCC	ATCC: CRL1660
Experimental Models: Organisms/Strains		
ZIKV Cambodian FSS13025 strain	World Reference Center for Emerging Viruses and Arboviruses at University of Texas Medical Branch, Galveston	FSS13025
C57BL/6NCrl	Charles River Laboratories	Strain 027
Mouse: *Mb21d*$^{-/-}$ (cGAS)	Herbert W. Virgin (PI). (Schoggins et al., 2014)	N/A
Mouse: B6(Cg)-*Ifnar1*$^{tm1.2Ees}$/J (*Ifnar1*$^{-/-}$)	The Jackson Laboratory	Stock No: 028288
Mouse: B6(Cg)-*Rag2*$^{tm1.1Cgn}$/J (*Rag2*$^{-/-}$)	The Jackson Laboratory	Stock No: 008449
Mouse: *Tlr7*$^{-/-}$ Mx1, *Mavs*$^{-/-}$ Mx1, and *Tlr7*$^{-/-}$ *Mavs*$^{-/-}$ *Mx1* mice	Akiko Iwasaki (PI) (Pillai et al., 2016)	N/A
Mouse: *Irf3*$^{-/-}$ *Irf7*$^{-/-}$	Tadatsugu Taniguchi (PI) (Honda et al., 2005)	N/A
Sequence-Based Reagents		
Primers against ZIKV NS5 (F: GGCCACGAGTCT GTACCAAA; R: AGCTTCACTGCAGTCTTCC).	This Paper	N/A
ZIKV IDT Primetime primer probe set (F: CCGCT GCCCAACACAAG; R: CCAC TAACGTTCTTTTGC AGACAT; probe, 50-/56-FAM/AGCCTACCT/ZEN/ TGA CAAGCAATCAGACACTCAA/3IABkFQ/-30)	(Lanciotti et al., 2008) Integrated DNA Technologies	N/A
Primers for mouse *Hprt* (F: GTTGGATACAGGCCA GACTTTGTTG; R: GAGGGTAGGCTGGCCTATTGGCT)	(Foxman et al., 2015)	N/A

CONTACT FOR REAGENTS AND RESOURCE SHARING

Requests for reagents will be fulfilled by the corresponding author Akiko Iwasaki (akiko.iwasaki@yale.edu).

EXPERIMENTAL MODEL AND SUBJECT DETAILS

Mice

C57BL/6NCrl (WT) female mice were purchased from Charles River Laboratories and subsequently bred and housed at Yale University. *Rag2*$^{-/-}$, *Ifnar1*$^{-/-}$, *Irf3*$^{-/-}$ *Irf7*$^{-/-}$ (Honda et al., 2005) (generous gift from Dr. T. Taniguchi), and *Mx1* (generous gift from Dr. P. Staeheli), *Tlr7*$^{-/-}$ *Mx1, Mavs*$^{-/-}$ *Mx1* and *Tlr7*$^{-/-}$ *Mavs*$^{-/-}$ *Mx1* mice (Pillai et al., 2016) were bred and housed at Yale

University. *Mb21d*$^{-/-}$ (cGAS knockout) mice (Schoggins et al., 2014) were a generous gift from Dr. Herbert W. Virgin. Ages of the mice used in the experiments are summarized in the Table S1. Pregnancy studies were timed by the presence of a plug, indicating gestational age E0.5. All animal procedures were performed in compliance with Yale Institutional Animal Care and Use Committee protocols.

Viruses

Aedes albopictus mosquito (C6/36) cells were maintained at 30°C in Dulbecco's Modified Eagle's Medium (GIBCO) supplemented with 10% heat-inactivated fetal bovine serum with penicillin/streptomycin (GIBCO) and 1% tryptose phosphate broth (Sigma). Vero cells were maintained at 37°C in Dulbecco's Modified Eagle's Medium (GIBCO) supplemented with 10% heat-inactivated fetal bovine serum with penicillin/streptomycin (GIBCO). ZIKV Cambodian FSS13025 strain was used for all studies. ZIKV stocks were propagated in C6/36 cells or Vero cells and titrated by plaque assay in Vero cells. The Cambodian isolate was obtained from the World Reference Center for Emerging Viruses and Arboviruses at University of Texas Medical Branch, Galveston. For high-titer doses, ZIKV was concentrated by ultracentrifugation (Beckman Optima LE-80K ultracentrifuge, SW28 rotor, 25,000 rpm, 5 hr).

METHOD DETAILS

In Vivo Infections

Intravaginal ZIKV infection was performed as follows: Virgin female mice were treated with Depo-Provera (Pfizer) 5 days prior to infeXction. No treatment was given to pregnant mice prior to infection. A Calginate swab (Fischer scientific) was used to remove mucous from the vaginal lumen, and mice were infected vaginally with 10-20 μl Cambodian ZIKV of indicated titer (2.5×10^4 PFU to 5.2×10^5 PFU) by using a pipette. For intraperitoneal infection, mice were infected with 1.5×10^5 PFU diluted in PBS and injected in a total volume of 500 μl. Vaginal washes were taken 1-7 days post-infection by first removing mucous using a Calginate swab then pipetting 50 μl of PBS in the vaginal lumen by using a pipet and added to 450 μl of PBS supplemented with 1% FBS, 10 mg/ml glucose, 0.5 μM $MgCl_2$ and 0.9 μM Ca Cl_2 to maintain viral infectivity and stored −80°C. Viral titers were determined by plaque assay on Vero cells or by isolating RNA from vaginal wash using RNeasy Mini Kit (QIAGEN). ZIKV titers were determined by normalization to RNA prep of virus stock. To measure ZIKV viremia, 50-100ul of blood was collected by retro-orbital bleed at indicated time points post-infection. Total blood RNA was extracted using Trizol (Thermo Fischer Scientific) extraction followed by purification with RNeasy Mini Kit (QIAGEN). To determine levels of virus in tissues of virgin and pregnant mice, mice were euthanized and indicated tissues were collected into RNAlater (QIAGEN). RNA was extracted using Trizol (Thermo Fischer Scientific). Mice were euthanized before reaching the moribund state due to humane concerns.

Quantification of ZIKV Genome by qRT-PCR

cDNA was synthesized using iScript cDNA synthesis kit (Bio-Rad). Quantitative PCR was performed using SYBR-Green (Bio-Rad) or PrimeTime master mix (Integrated DNA Technologies) on a CFX Connect instrument (Bio-Rad). ZIKV RNA was detected using primers designed to NS5 (F: GGCCACGAGTCTGTACCAAA; R: AGCTTCACTGCAGTCTTCC). ZIKV RNA was also confirmed using a previously published primer set (Lanciotti et al., 2008): F: CCGCTGCCCAACACAAG; R: CCAC TAACGTTCTTTTGCAGACAT; probe, 50-/56-FAM/AGCCTACCT/ZEN/TGA CAAGCAATCAGACACTCAA/3IABkFQ/-30 (Integrated DNA Technologies). ZIKV RNA levels were normalized to *Hprt* (F: GTTGGATACAGGCCAGACTTTGTTG; R: GAGGGTAGGCTGGCCTATTGGCT) (Foxman et al., 2015) for blood and organ samples. For vaginal washes, limit of detection was determined by dilution of the standard curve (purified ZIKV genomic RNA) to a value where Ct values were no longer amplified. For tissue and blood samples, limit of detection was determined by calculating the 'Relative ZIKV Value' for the highest Ct value (36) amplified specifically and consistently for the NS5 primer set and the average *Hprt* value for that sample type.

Quantification of ZIKV by Plaque Assay

For plaque assays, vaginal wash samples were serially diluted prior to infection of Vero cells. Plaque assays were overlayed with 2% agarose, and 5 days later, cells were fixed with 10% formalin and stained with 0.005% amido black (MP Biochemicals).

Electron Microscopy

The embryos were emerge fixed in 4% paraformaldehyde, and 5% glutaraldehyde, then 100 micron thick sections were cut on a Vibrotome. The sections were incubated in mouse anti NS1 antibody (1:5000) followed by biotinylated anti mouse secondary antibody (Vector BA-2000) and Vectastain Elite ABC (Vector PK-6100). Monoclonal antibody 17A12-1G5, which was originally raised against DENV-2 NS1, was found to cross-react with all ZIKV strains used in these studies. To visualize, we used the glucose-oxidase-DAB-nickel method. The sections then were treated in ascending alcohols, and embedded in Durcupan ACM (EMS14040). 70 nm ultrathin sections were cut on Leica ultramicrotome, and the images were collected on FEI TEM. The analysis was carried out in a blinded manner.

QUANTIFICATION AND STATISTICAL ANALYSIS

Data Analysis

Data analysis was performed using GraphPad Prism and Microsoft Excel. A one-tailed student t test was used to determine significance of fetal weights and 6 hr versus 24 hr vaginal washes. A spearman rank correlation coefficient was used to compare the plaque assay and RT-qPCR values for vaginal washes. Data are represented as mean ± SEM or as individual data points, as stated in the figure legends. Number of replicates and animals for each experiment are enclosed in their respective figure legends.

Cell

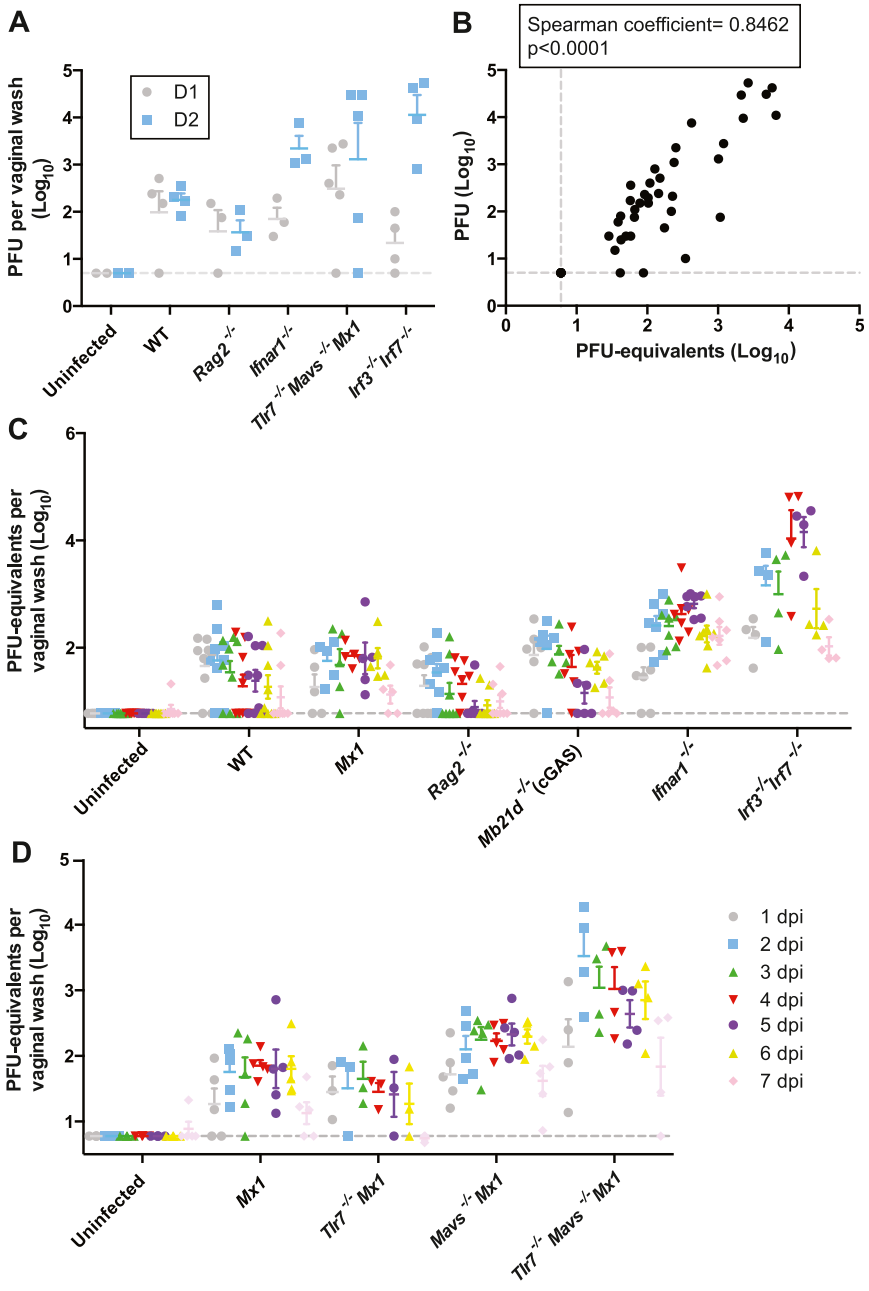

Figure S1. Vaginal Infection of Virgin Female Wild-Type Mice Leads to Viral Replication in the Vaginal Mucosa, Related to Figure 1

Virgin female mice of the indicated genotypes were infected with 2.5 × 10^4 PFU of Cambodian ZIKV intravaginally.

(A) Plaque assays were performed of vaginal washes taken 1 and 2 dpi.

(B) Plaque forming units were plotted against RT-qPCR values for individual mice. Spearman coefficient is 0.85 and p value of < 0.0001.

(C) Individual values for PFU-equivalent levels of ZIKV RNA from vaginal washes corresponding to Figure 1A are shown.

(D) Seven- to 9-week-old virgin female mice of the indicated genotypes were infected with 2.5 × 10^4 PFU of Cambodian ZIKV intravaginally. On the indicated days post-infection, vaginal washes were collected and viral load was analyzed by RT-qPCR.

(A and B) Results shown are mean ± SEM involving uninfected (n = 2), *Ifnar1*$^{-/-}$ (n = 3), WT (n = 4), *Rag2*$^{-/-}$ (n = 4), *Irf3*$^{-/-}$ *Irf7*$^{-/-}$ (n = 4) and *Tlr7*$^{-/-}$ *Mavs*$^{-/-}$Mx1 (n = 5) mice. For (C), results shown are mean ± SEM involving uninfected (n = 7), WT (n = 9), Mx1 (n = 5), *Rag2*$^{-/-}$ (n = 8), *Mb21d*$^{-/-}$ (cGAS) (n = 6), *Ifnar1*$^{-/-}$ (n = 7), and *Irf3*$^{-/-}$ *Irf7*$^{-/-}$ (n = 4) mice pooled from two independent experiments. For (D), results shown are mean ± SEM involving uninfected (n = 5), Mx1 (n = 5), *Tlr7*$^{-/-}$ *Mx1* (n = 3), *Mavs*$^{-/-}$ *Mx1* (n = 5), and *Tlr7*$^{-/-}$ *Mavs*$^{-/-}$*Mx1* (n = 4). Uninfected and *Mx1* mice from (D) are some of the same mice in (C). The gray dashed line indicates limit of detection.